

Cell Reports, Volume 32

Supplemental Information

Beaver and Naked Mole Rat Genomes

Reveal Common Paths to Longevity

Xuming Zhou, Qianhui Dou, Guangyi Fan, Quanwei Zhang, Maxwell Sanderford, Alaattin Kaya, Jeremy Johnson, Elinor K. Karlsson, Xiao Tian, Aleksei Mikhailchenko, Sudhir Kumar, Andrei Seluanov, Zhengdong D. Zhang, Vera Gorbunova, Xin Liu, and Vadim N. Gladyshev

Supplemental Information

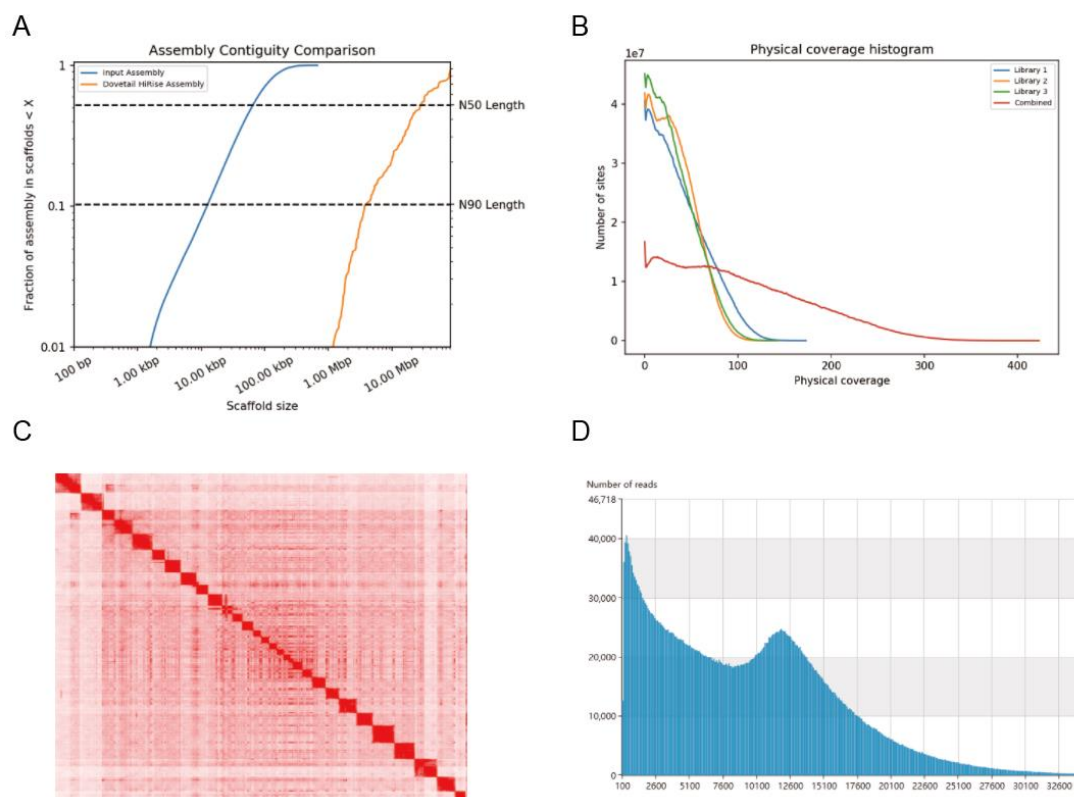


Figure S1, Related to Figure 1. Improvement of beaver and NMR genome assemblies.

(A) The two curves show a fraction of total length of the assembly present in scaffolds of a given length or smaller. Fraction of the assembly is indicated on the Y-axis, and the scaffold length in base pairs is given on the X-axis. Two dashed lines mark N50 and N90 lengths of each assembly. Scaffolds less than 1 kb were excluded. (B) Histogram of physical coverage over input assembly of the beaver Dovetail library. Coverage values are calculated as the number of read pairs with inserts between 1 and 100 kb spanning each position in the input assembly. (C) Contact matrices generated by aligning the Hi-C dataset to the final NMR assembly generated by 3D-DNA. Pixel intensity in the contact matrix indicates how often a pair of loci co-locate in the nucleus. (D) Sequence length distribution of NMR subreads. Sequence length is shown on the X axis, and read number of the Y axis.

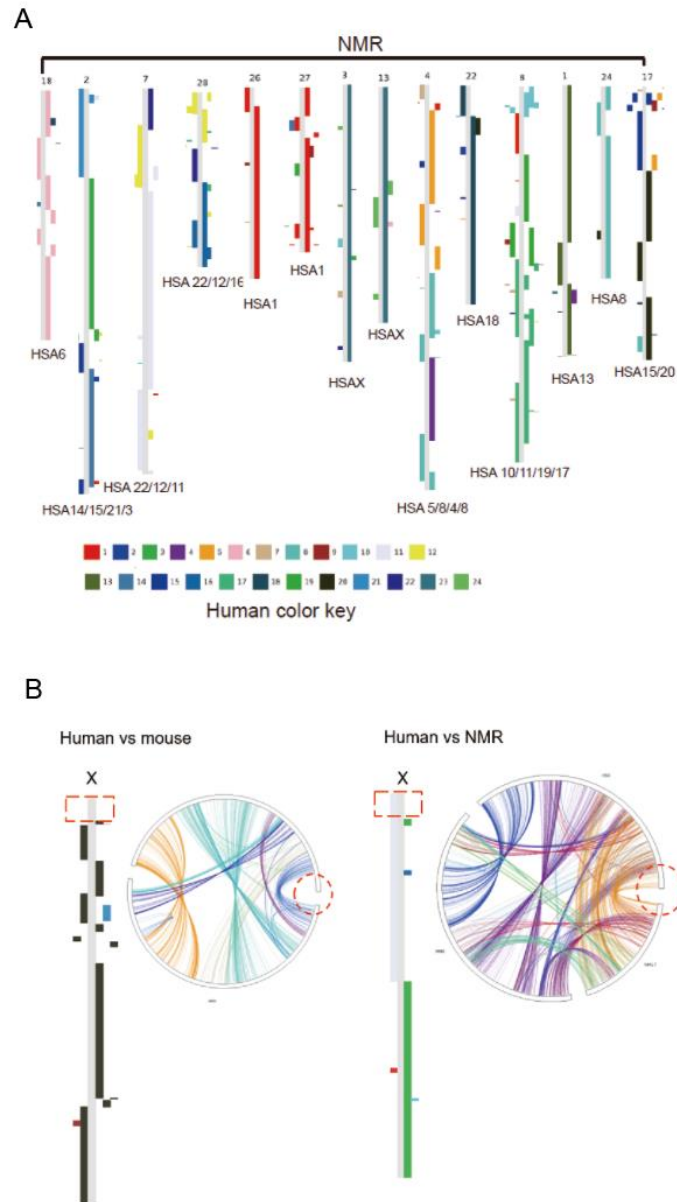


Figure S2, Related to Figure 1. Genome synteny among NMR, human and mouse.

(A) Synteny between several human chromosomes (HSA 6, 15/14, X, 1, 10/1, 12/22, 13, 8, 18, 8/4/8, 15/20) and NMR superscaffolds proposed in the putative rodent ancestor genome architecture. (B) Synteny between human chromosomes (X, Y), and mouse and NMR assemblies.

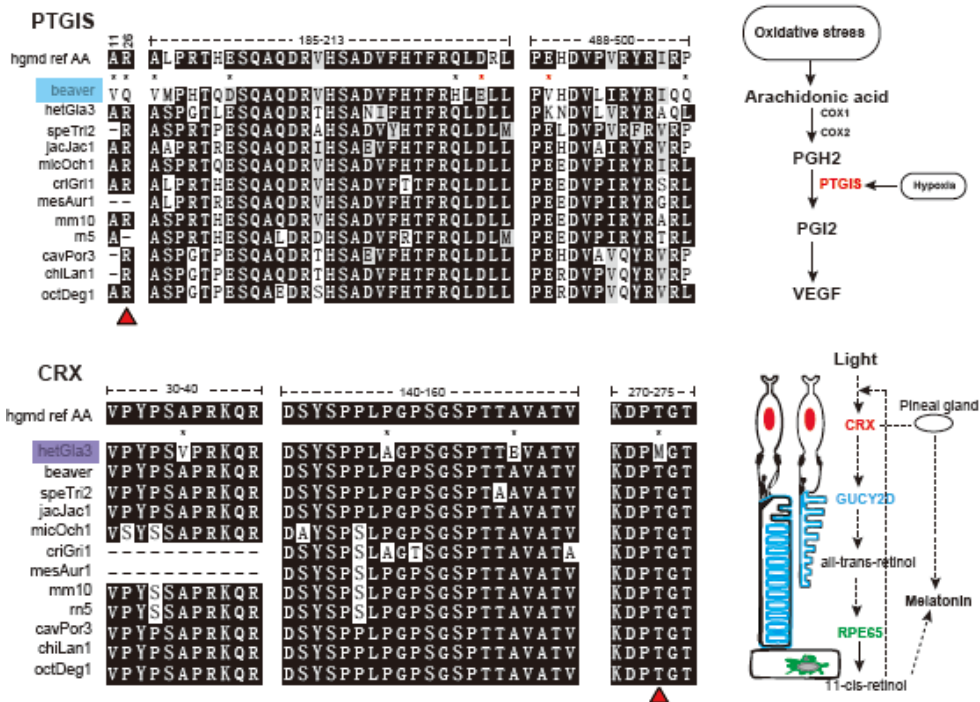


Figure S3, Related to Figure 2. Protein sequence alignments of PTGIS and CRX that harbor disease-causing, unique, and positively selected sites in the beaver and NMR.

Schematic representation of the roles of PTGIS in response to oxidative stress and hypoxia as well as the role of CRX in sensing light is shown on the right of the alignments.

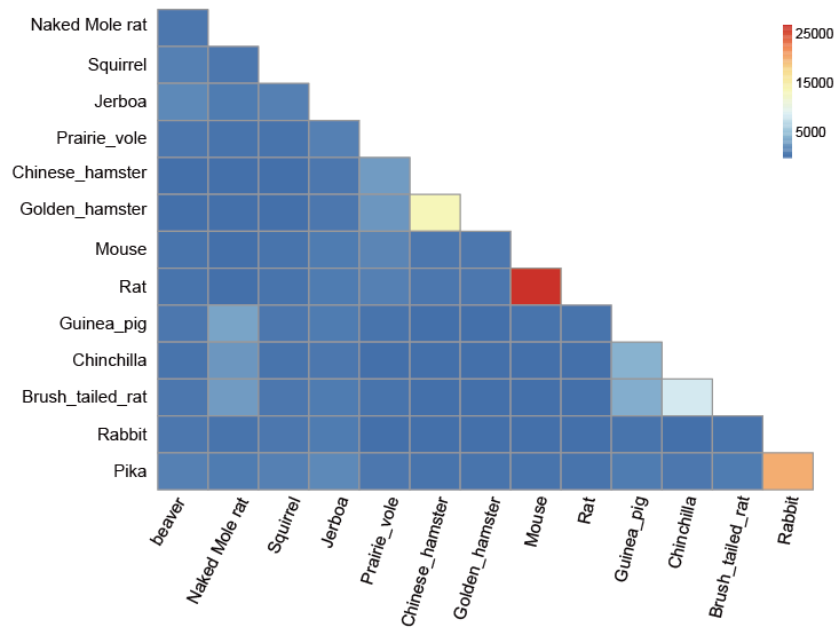


Figure S4, Related to Figure 3. Heatmap of unique substitutions across all pairs of analyzed rodents in the current study.

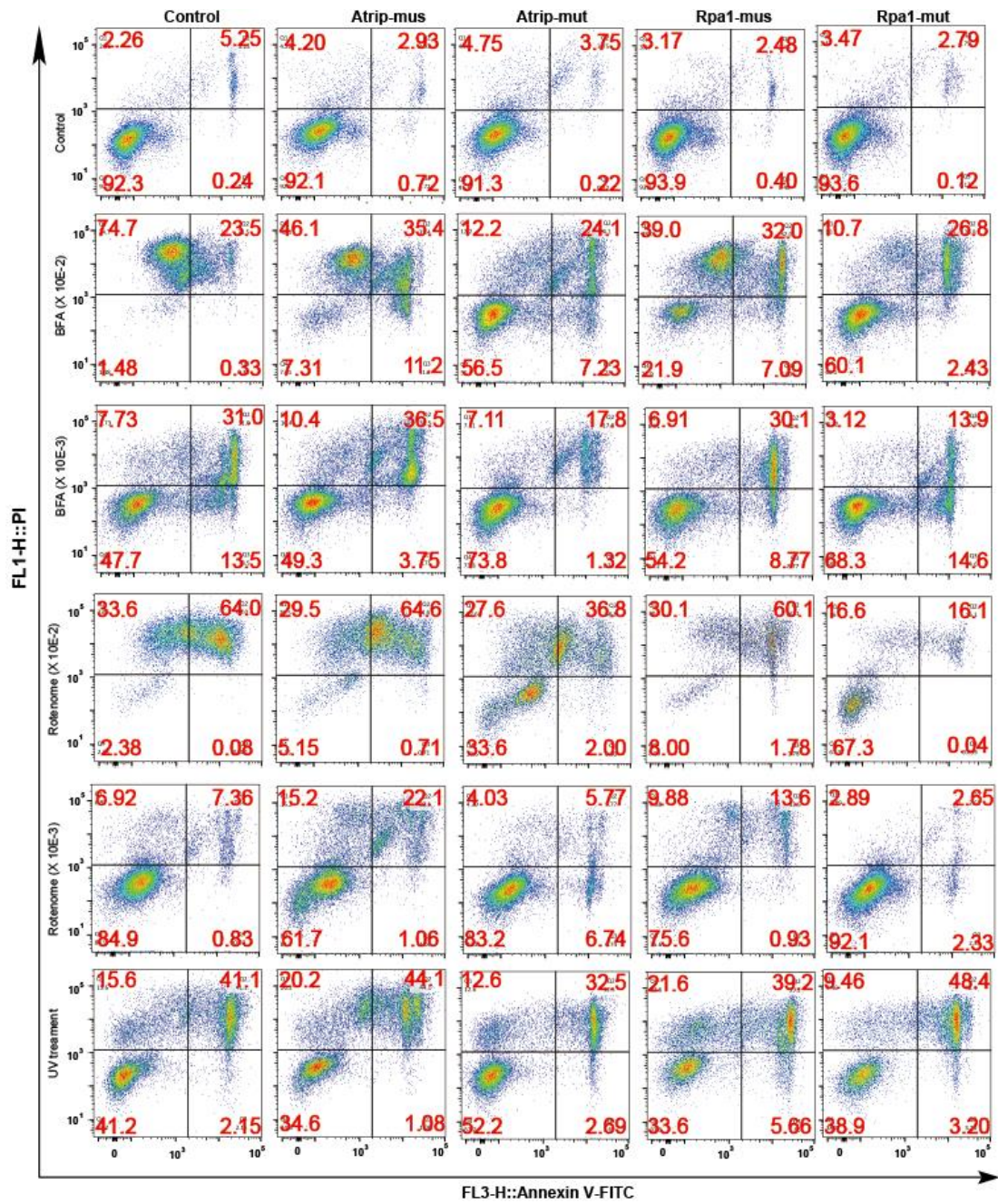


Figure S5. Related to Figure 3. Comparison of apoptotic rate of cells carrying control proteins or mutant versions (Ser618Ile in Atrip, Thr572Met in Rpa1) following treatment of cells with UV irradiation, rotenone and Brefeldin A for 48 h.

Analyses were carried out by using flow cytometry.